Research Article

Nano Biomed Eng

Antibacterial Activity and Characterization of Chitosan Nanoparticles Prepared from Hijau Lumut Banana (*Musa paradisiaca* L.) Peel Ethyl Acetate Extract

Wiwik Susanah Rita, Ni Kadek Linda Erika Yanti, I. Made Dira Swantara

Department of Chemistry, Faculty of Mathematics and Natural Sciences, Udayana University, Bali, Indonesia

Corresponding author. E-mail: susanah.rita@unud.ac.id

Received: Jul. 11, 2022; **Revised:** Nov. 24, 2022; **Accepted:** May 24, 2023

Citation: W.S. Rita, N.K.L.E. Yanti, I.M.D. Swantara. Antibacterial activity and characterization of chitosan nanoparticles prepared from Hijau lumut banana (*Musa paradisiaca* L.) peel ethyl acetate extract. *Nano Biomedicine and Engineering*, 2023, 15(3): 278−287.

http://doi.org/10.26599/NBE.2023.9290022

Abstract

Peels of Hijau lumut banana (HLB) (*Musa paradisiaca* L.) are a form of organic waste that has not been widely utilized. This study was conducted to determine the antibacterial activity of ethyl acetate extract of HLB peels and that of their nanoparticles at various concentrations of chitosan against *Staphylococcus aureus* and *Escherichia coli*. It was also aimed to characterize the most active nanoparticles. Extraction of HLB peels was carried out by maceration and partitioning methods. Ionic gelation was applied to synthesize nanoparticles using chitosan crosslinked with sodium tripolyphosphate (NaTPP). Antibacterial activity assay was carried out by the agar diffusion well method. The nanoparticles were characterized by the following analyses: determination of their size distribution and zeta potential by a particle size analyzer, and of their morphology by scanning electron microscopy and transmission electron microscopy, phytochemical screening to determine secondary metabolite contents, determination of retention factor values and staining patterns by thin-layer chromatography, ultraviolet–visible (UV–Vis) spectrophotometry to confirm nanoparticle formation, and determination of the characteristics of their functional groups by Fourier transform infrared spectrophotometry. The antibacterial activity assay showed that the nanoparticles exhibited a stronger antibacterial activity than the ethyl acetate extract, with chitosan at a concentration of 1% being associated with the highest activity. In terms of their morphology, the nanoparticles were amorphous (non-uniform), while they absorbed UV–Vis at 385 nm and had the following functional groups: —OH, —NH, —CH, and P—O. This study revealed that these nanoparticles exert antibacterial effects and the secondary metabolites were encapsulated via crosslinking between chitosan and NaTPP.

Keywords: antibacterial activity; banana peel; chitosan; *Escherichia coli*; nanoparticle; *Staphylococcus aureus*

Introduction

Banana is a valuable plant for human use, with all parts of banana plants having beneficial health effects, such as ameliorating diarrhea, tonsillitis, hemorrhoids, and dysentery. The medicinal value of banana plants is because they contain secondary metabolites such as tannins, alkaloids, and saponins [1].

The peel is one part of banana with potential medicinal uses, but it is currently typically discarded because only the flesh of the fruit is consumed. This highlights the need for research on the potential of banana peel as a medicinal agent.

Humans regularly suffer from bacterial infections, with *Escherichia coli* and *Staphylococcus aureus* infections being particularly common. Hijau lumut banana (HLB) peel is known to have an antibacterial activity. Indeed, it has been reported that methanol extract of HLB (*Musa paradisiaca* L.) peel inhibited *S. aureus* and *E. coli* with inhibitory zones of 12.25 and 10.25 mm, respectively, at a concentration of 20% [2]. Based on the results of a preliminary test, it was found that partitioned extracts, namely, n-hexane, ethyl acetate, and n-butanol extracts, at a concentration of 20% could inhibit the growth of *S. aureus* with inhibitory zones of 9.50, 15.50, and 11.25 mm, respectively, while for *E. coli* the inhibitory zones were 8.75, 12.50, and 10.50 mm in diameter. Meanwhile, the aqueous extract did not inhibit the growth of either bacterium.

The results of the antibacterial activity assay of banana peel showed that the ethyl acetate extract was the most active. Under a classification scheme where an inhibition zone of less than 5 mm reflects weak activity, 5–10 mm reflects a moderate activity, 10–20 mm reflects a strong activity, and greater than 20 mm reflects a very strong activity [3]. The ethyl acetate extract was allocated into the strong category, but its activity can potentially be increased further. The activity may be impeded by several factors, such as a large particle size [4]. A large particle size causes a decrease in activity against bacteria because a larger particle size is associated with a relatively small surface area, meaning that the contact between the particles and bacteria is not optimal [5].

In this context, the antibacterial activity can be increased by a nanotechnological approach. Herbal medicines optimized by nanotechnology have outstanding advantages over conventional formulations of the active ingredients of plant extracts, including increased solubility and bioavailability, enhanced stability, continuous delivery, increased distribution of tissue macrophages, protection from toxicity, increased pharmacological activity, and protection from physical and chemical degradation [6, 7]. Verma et al. [8] stated that green nanotechnology in phytoformulations, greatly helps to the environmental sustainability without endangering human health or the environment. In addition, Nyoni et al. [9] reported the antibacterial activity of silver nanoparticles prepared from extracts of *Sclerocarya birrea* leaf and stem bark, which were found to exert antibacterial activity against *E. coli* and *S. aureus*. Moreover, Kumar et al. [10] synthesized CaO nanoparticles by precipitation techniques using calcium chloride and sodium hydroxide. These nanoparticles were characterized for their structure, morphology, chemical composition, and optical behavior using Fourier transform infrared (FTIR) spectroscopy. The CaO nanoparticles have been synthesized in a cubic crystalline structure with an average crystallite size of about 13 nm, and they exhibit an aggregated morphology of nanoclusters. The FTIR and energy-dispersive X-ray spectroscopy (EDS) spectra show that the nanoparticles are successfully generated from the chemical recipe of the precipitation process due to the existence of unique peaks.

The ionic gelation method is often used in making nanoparticles employing a chitosan biopolymer that is crosslinked with sodium tripolyphosphate (NaTPP). The advantage of this method is that the process is relatively easy to perform and does not involve high temperatures, so it does not damage the active compounds [11]. Chitosan nanoparticles are natural materials with excellent antimicrobial and physicochemical properties, have a wide range of bioactivities, and are environmentally friendly. In the synthesis of chitosan nanoparticles, electrostatic interactions occur between the amine group of chitosan and negatively charged polyanion groups such as tripolyphosphate. Chitosan can be dissolved in acetic acid in the presence or absence of a stabilizer [12]. Owing to these advantages of chitosan nanoparticles, this study is aimed to synthesize such nanoparticles prepared from HLB peels, in order to increase their antibacterial activity, and to characterize them.

Experimental

Plant preparation

HLB peels were cleaned and dried at room temperature for 7 days. The dried peels were then blended and sieved through a 60 mesh.

Determination of water content

An empty porcelain dish with a lid was heated at

105 ℃ for 1 h and then weighed. The heating was repeated several times until the mass remained constant (m_0). One gram of peel powder was added to the dish, weighed m_1, and then heated again to a constant mass (m_2). The maximum moisture content of the dry sample was 10% [13]. The formula for the percentage water content m_{water} is as follows:

$$m_{water} = \frac{m_1 - m_2}{m_1 - m_0} \times 100\%$$

where m_0 is the mass of dish and lid, m_1 is the mass of dish, lid, and sample before drying, and m_2 is the mass of dish, lid, and sample after drying.

Extraction

One kilogram of HLB peel powder was extracted for 72 h by a maceration method using methanol, followed by filtering with filter paper. The resulting filtrate was evaporated using a rotary vacuum evaporator until a concentrated methanol extract was obtained. The crude extract was then dissolved in 70% methanol and re-evaporated to remove the methanol to obtain a water extract. The aqueous extract was then partitioned with n-hexane and ethyl acetate. The ethyl acetate filtrate was re-evaporated to obtain a concentrated extract of ethyl acetate [2].

Nanoparticle synthesis

One gram of ethyl acetate extract was dissolved in 35 mL of ethanol and supplemented with 15 mL of distilled water, followed by mixing with 50 mL of chitosan solution in 1% glacial acetic acid. Then, 50 mL of NaTPP solution was added in a dropwise manner and stirred using a magnetic stirrer at 3 800 r/min for 2 h. The colloidal nanoparticles formed were centrifuged for 15 min at 3 000 r/min. The precipitated nanoparticles were put into a freezer and allowed to stand for 2 days, after which they were dried with an air cooler and then ground using a mortar and pestle [14]. The nanoparticles were made into three different chitosan concentrations: 1%, 2%, and 4%.

Antibacterial assay

Both *S. aureus* and *E. coli* growing on nutrient agar were scratched using a needle and then placed in 50 mL of nutrient broth. They were subsequently placed in an incubator at 37 ℃ for 24 h. Antibacterial activity assay was carried out on ethyl acetate extract and its nanoparticles using the agar diffusion well method. The nutrient agar in liquid form was put into a sterile Petri dish, after which 200 μL of bacterial suspension was added, followed by shaking and then being left to solidify. Diffusion wells were made using a 0.5 cm cork borer, followed by sterilization by passing over a Bunsen flame and then being pressed into the medium to form a diffusion well. Twenty microliters of ethyl acetate extract and its nanoparticles, as well as a negative control (Tween-80 at a concentration of 10%) and positive control (0.03% amoxicillin), were each put into a diffusion well and incubated for 24 h at 37 ℃. The diameter of the clear zone formed was measured.

Nanoparticle characterization

The most active nanoparticles were characterized using a particle size analyzer (PSA) (SZ-100; Horiba Scientific, Tokyo, Japan), scanning electron microscopy (SEM, SEM-EDS, JSM-6510LA; JEOL, Japan), transmission electron microscopy (TEM, JEM2100, JEOL), phytochemical screening, thin-layer chromatography (TLC), ultraviolet–visible (UV–Vis) spectrophotometry (Shimadzu, Japan), and FTIR spectrophotometry (Shimadzu, Japan). PSA was used to measure the size of the formed particles and zeta potential value, while SEM was applied to determine the morphology of the powder. A phytochemical assay was carried out to identify the contents of secondary metabolites, such as alkaloids, triterpenoids, steroids, flavonoids, phenols, and saponins [15]. TLC was used to determine the stability of the compounds both before and after being made into nanoparticles, UV–Vis-spectrophotometry ensured the successful formation of samples, and FTIR spectroscopy characterized the functional groups of nanoparticles.

Results and Discussion

Determination of water content and extraction

The water content of HLB peel powder was 7.88% ± 0.45%. This value is below 10%, which is important as moisture content greater than 10% causes a humid environment in which microbes can grow and reduces the stability of the extract [16]. Maceration of a 1 kg sample yielded 144 g of methanol extract with a blackish brown color, and the yield percentage was 14.4%. The yield percentage can be influenced by several factors, including temperature, duration of

maceration, and the type of solvent used [17]. A total of 128 g of concentrated extract was dissolved in a 7∶3 ratio of methanol and water with a total volume of 1.2 L. The extract was then evaporated with a rotary vacuum evaporator to remove the methanol, to obtain a water extract. This procedure was intended to facilitate the partitioning process. If the extract still contains methanol, then no separation occurs when partitioned with ethyl acetate. The next process was partitioning using n-hexane solvent first. This was performed because n-hexane is a non-polar solvent and can extract oil and fat in the extraction process [18], so it does not interfere with subsequent partitioning with ethyl acetate solvent. The yield of the ethyl acetate extract was 10.15%.

Synthesis of nanoparticles

The synthesis of nanoparticles of ethyl acetate extract of HLB peel was carried out by the ionic gelation method by adding NaTPP as a polyanion, which can crosslink with chitosan. Chitosan was chosen because it can reduce the side effects of drugs and prolong the duration of drug activity. Dilute acid was used for dissolving chitosan in order to obtain cations from chitosan, namely, the amine group. This amine group forms crosslinks with the NaTPP polyanion [19]. NaTPP salt is used as a crosslinking agent because it tends not to be toxic, so this additive has been approved by the US Food and Drug Administration [20]. The synthesis of the nanoparticles was carried out using three different concentrations of chitosan, namely, 1%, 2%, and 4%. This was intended to determine the effect of chitosan on the antibacterial activity produced. The mass of the resulting nanoparticles is presented in Table 1.

Table 1 Mass of nanoparticles from ethyl acetate extract of HLB peel in various chitosan concentrations

Chitosan concentration (%)	Dry nanoparticle mass (g)	Nanoparticle color
1	0.59 ± 0.24	Dark brown
2	1.48 ± 0.17	Brown
4	1.84 ± 0.19	Brown

Table 1 shows that the mass of the resulting nanoparticles increases with increasing chitosan concentration. The reaction mechanism formed in the synthesis of nanoparticles is based on the interaction between the positive charge of chitosan and the negative charge of NaTPP. Polycationic chitosan was dissolved using acetic acid, and polyanion NaTPP was formed due to its dissociation in water to form OH^- and $P_3O_{10}^{5-}$ ions, which then reacted with NH_3^+ from chitosan [21]. The cross-reaction that occurred between chitosan and NaTPP can be seen in Fig. 1.

Antibacterial assay

The assays on the antibacterial effects of ethyl acetate extract against *S. aureus* and *E. coli* revealed inhibitory zones of (15.77 ± 0.25) mm and (12.90 ± 0.43) mm, respectively. The results of the antibacterial assays of nanoparticles with various concentrations of chitosan are presented in Table 2.

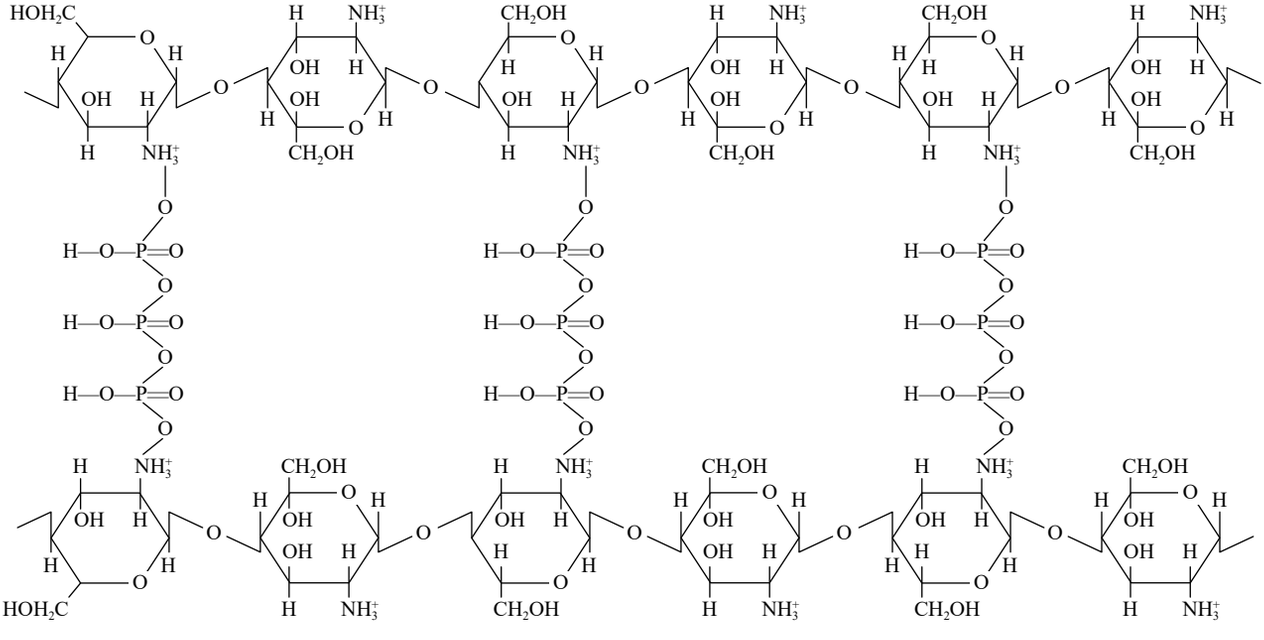

Fig. 1 Crosslinking reaction of chitosan nanoparticles with tripolyphosphate salt [22].

Table 2 Results of antibacterial activity assay of nanoparticles in various concentrations of chitosan against *Staphylococcus aureus* and *Escherichia coli* at a concentration of 200 g/L

Chitosan concentration (%)	Inhibitory zone (mm)	
	S. aureus	*E. coli*
1	20.55 ± 0.30	16.58 ± 0.25
2	18.10 ± 0.31	15.25 ± 0.25
4	16.28 ± 0.26	14.38 ± 0.34
Positive control (amoxicillin 0.03)	30.20 ± 0.30	27.01 ± 0.47
Negative control (Tween 10)	0.00 ± 0.00	0.00 ± 0.00

The results in Table 2 indicate that the nanoparticles from the ethyl acetate extract had a higher antibacterial activity than the ethyl acetate extract. This was due to several factors, including the surface area of the nanoparticles produced being larger than the particle in the ethyl acetate extract. Nanoparticles have a large surface area and a large number of atoms on their surface, so they have a low surface energy and surface tension, making it easier for particles to penetrate cell membranes [23]. Another factor is the presence of chitosan. Chitosan can inhibit bacteria by attaching to the bacterial cell wall to form a polymer membrane that can prevent nutrients from entering the bacterial cell, leading to cell death [24]. This is in line with the results of this study, where chitosan inhibited both bacteria; therefore, the antibacterial effect resulting from the use of chitosan in the nanoparticles was not negligible [25]. A graph comparing the antibacterial activities of each concentration of chitosan against the two bacteria is presented in Fig. 2.

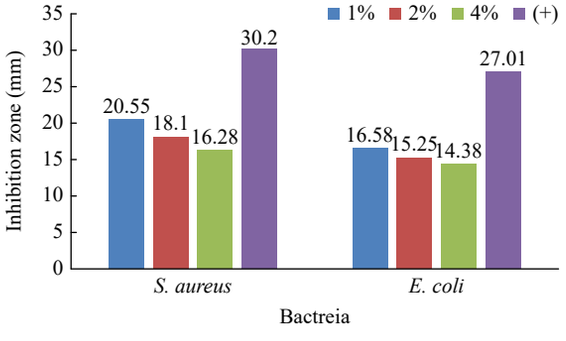

Fig. 2 Comparison of antibacterial activity with various concentrations of chitosan against *S. aureus* and *E. coli*.

Figure 2 shows that with an increasing concentration of chitosan, the antibacterial activity decreased. This is because chitosan tends to agglomerate at higher concentrations with a constant amount of NaTPP. The high concentration resulted in the particles formed from the reaction between chitosan and NaTPP being very large and dense, so that they grouped together to form aggregates and agglomerated. This agglomeration increased the particle size and led to a smaller surface area [26]. Characterization of nanoparticles was carried out under the conditions associated with the highest antibacterial activity (concentration of chitosan: 1%).

Characterization of nanoparticles

The nanoparticles were characterized in terms of nanoparticle size (using PSA), nanoparticle morphology (using SEM and TEM). The effectiveness of nanoparticle encapsulation was by comparing the content of compounds in the ethyl acetate extracts and their nanoparticles using phytochemical screening, and the numbers of spots in TLC analysis, UV–Vis analysis, and functional group analysis with FTIR.

Nanoparticle size was measured using PSA. The nanoparticles have an average size of (956.4 ± 23.8) nm with a zeta potential of (−20.40 ± 0.65) mV. The size of the nanoparticle is in accordance with Singh et al. [27], namely nanoparticles are small particles with all three dimensions measuring less than 1 μm.

Several factors that affect particle size include concentration, numbers of chitosan and NaTPP molecules, and the preparation method was used in Ref. [28]. The zeta potential value indicates that the nano ethyl acetate extract of HLB peel has the ability to deliver bioactive substances [29]. Particle size and polydispersity index values are shown in Fig. 3.

The value of the polydispersity index generated in this study was almost 0.7. The deviation of the particle size that was close to this maximum limit allows some particles to agglomerate more rapidly due to the lack of other stabilizers such as surfactants that can prevent faster agglomeration [30]. The peaks in the curve in Fig. 3 represent the area of the particle size distribution. The curve in Fig. 3 forms two peaks, which indicates that the nanoparticle size does not

have a good uniformity. Good curve uniformity is indicated by a curve that only forms a single peak [30].

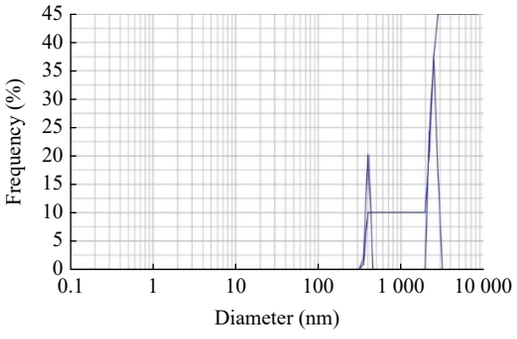

Fig. 3 Particle size distribution curves of nanoparticles.

Nanoparticle morphology was analyzed using SEM. The morphology of the most active ethyl acetate extract nanoparticles is presented in Fig. 4. In terms of their morphology, the nanoparticles have an amorphous (non-uniform) shape, with an imperfect round shape, an imperfect oval shape, and corners in each particle. The chemical composition on the surface of the most active nanoparticles is presented in Table 3.

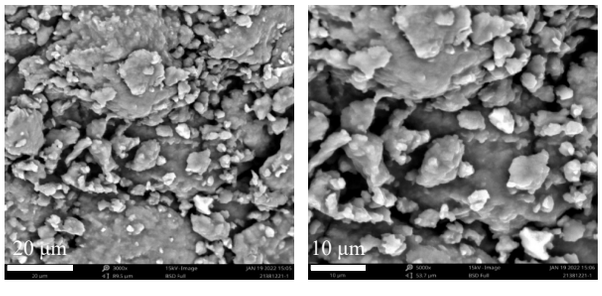

Fig. 4 Morphology of the nanoparticles using SEM. **(a)** 3 000× magnification; **(b)** 5 000× magnification.

Table 3 Surface chemical composition of the nanoparticles at 5 000× magnification using EDS

Element number	Element symbol	Element	Concentration (%)
8	O	Oxygen	41.53
6	C	Carbon	37.48
7	N	Nitrogen	11.69
15	P	Phosphorus	6.95
11	Na	Sodium	1.91
14	Si	Silicon	0.36
13	Al	Aluminum	0.08

The chemical composition based on EDS consists of carbon (C) (41.53%), oxygen (O) (37.48%), and nitrogen (N) (11.69%) as the main components. This indicates the formation of nanoparticles in the presence of a chitosan biopolymer with the chemical formula $(C_6H_9NO_3)_n$, NaTPP, and the active compound contained in the ethyl acetate extract. Other elements such as Na, P, Si, and Al were found at low levels, while hydrogen (H) was not detected by EDS. This is most likely because hydrogen is lighter than the other elements, so it is located above the surface and is not detected [31].

The characterization by TEM provides information about the morphology of the nanoparticles. Figure 5 shows that the morphology of the ethyl acetate extract at the nanoscale was not perfectly round, which indicates that the bioactive substance from the HLB peel extract had been encapsulated in nano-chitosan. Chitosan is more soluble under acidic conditions, so it can increase the porosity of the formed chitosan-tripolyphosphate; when it combines with the ethyl acetate extract of HLB peel, the morphology expands. This indicates that the extract was deposited on the chitosan-tripolyphosphate surface [32].

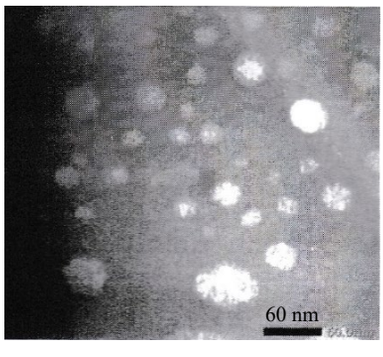

Fig. 5 Nanoparticle characterization by TEM.

Phytochemical screening results of ethyl acetate extract and its nanoparticles are shown in Table 4. The data showed that the secondary metabolites of the alkaloid group were not detected in the nanoparticles, presumably because only a few of the alkaloid compounds in the ethyl acetate extract were successfully encapsulated during the preparation of the nanoparticles with chitosan and NaTPP, but other secondary metabolites could still be found in the nanoparticles. This indicates that the active compound was the ethyl acetate extract successfully encapsulated in the nanoparticles, so that it could still function as an antibacterial. Similar results were also obtained by Nurviana [33], who also found groups of flavonoid compounds, tannins, polyphenols, triterpenoids, and quinones in limus seed extract and nanoparticle preparations of limus seed extract.

Table 4 Results of phytochemical screening of ethyl acetate extract and its nanoparticles of HLB peels

Secondary metabolites	Ethyl acetate extract	Nanoparticles
Alkaloid	(+)	(−)
Phenolic compound	(+)	(+)
Flavonoids	(+)	(+)
Terpenoids	(+)	(+)
Saponins	(−)	(−)

The results of the TLC analysis showed that the retention factor (Rf) values of the ethyl acetate extract and the nanoparticles had some similarities. A chromatogram of ethyl acetate extract and nanoparticles is presented in Fig. 6. Based on this chromatogram, the Rf values were obtained, as shown in Table 5.

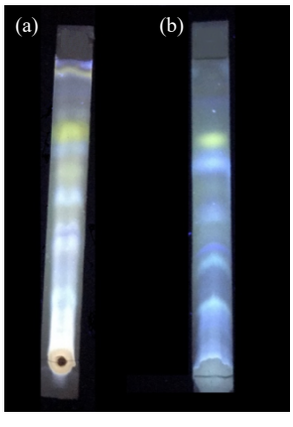

Fig. 6 Chromatogram of **(a)** HLB peel ethyl acetate extract and **(b)** nanoparticles.

Table 5 Rf values of HLB peel ethyl acetate extract and its nanoparticles

Stains	Rf value	
	Ethyl acetate extract	Nanoparticles
1	0.35	0.37
2	0.41	0.39
3	0.45	0.42
4	0.52	0.49
5	0.56	—
6	0.64	0.63
7	0.68	0.68
8	0.98	—
9	0.99	—

The similarity of the Rf values indicated that some of the ethyl acetate extract compounds were successfully encapsulated in the nanoparticles. Several factors affect the undetectable component with TLC including sorbent quality, humidity, plate thickness, elution distance, and ambient temperature [34]. Another factor that can exert an influence is the method of nanoparticle preparation, where some particles agglomerate and condense. This agglomeration causes the compound content in the ethyl acetate extract to not be completely encapsulated in the nanoparticles [30].

The UV–Vis-spectrophotometry results for characterizing the nanoparticles are presented in Fig. 7. The spectrum of the nanoparticles of the ethyl acetate extract shows a peak at a wavelength of 386 nm. This is probably due to the content of secondary metabolites in the extract, where it is possible that electrons are excited from π to π*. These compounds are a group of flavonoids or phenolic groups that have aromatic groups where the electrons experience delocalization. This is in accordance with the results of the phytochemical analysis (Table 3), which revealed the presence of these compounds. Duraisamy et al. [35] reported that the UV–Vis spectrum of pure chitosan particles shows a peak at 339 nm, representing a shift to a longer wavelength (bathochromic) in the nanospectrum. This proves that the secondary metabolites have been encapsulated in chitosan containing a —NH_2 group, resulting in the excitation of electrons from n to π* and an extension of electron delocalization.

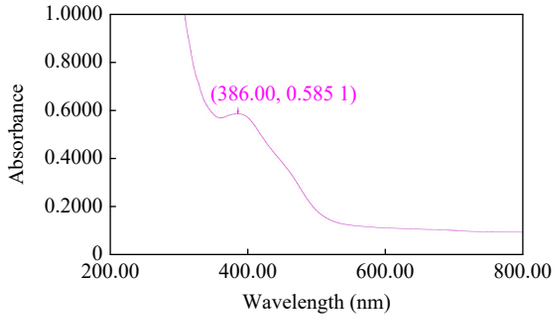

Fig. 7 UV–Vis spectrum of nanoparticles of ethyl acetate extract of HLB peel.

The FTIR analysis displays a number of peaks associated with numerous functional groups. The characterization of nanoparticles of ethyl acetate extract of HLB peel by FTIR can reveal the presence of changes in functional groups that indicate the occurrence of chemical interactions. The interaction due to the crosslinks formed between the HLB peel ethyl acetate extract with chitosan and NaTPP can be seen through the shift in the wavenumber and the intensity of the peaks [36]. The spectrum of chitosan and nanoparticles of HLB peel using FTIR can be seen in Fig. 8.

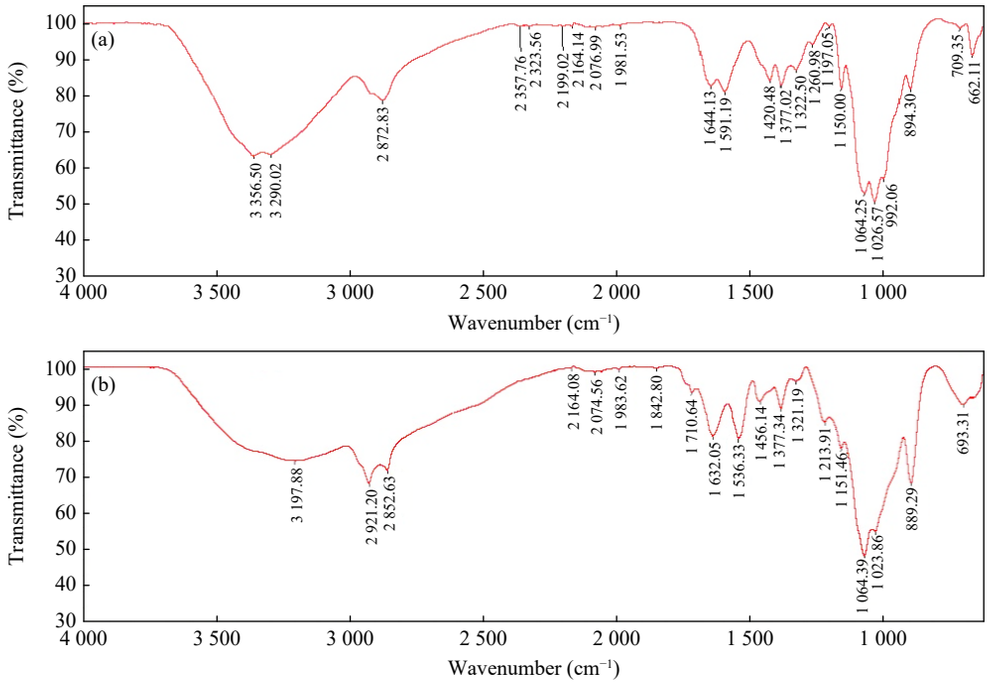

Fig. 8 FTIR spectrum. **(a)** Chitosan; **(b)** nanoparticles of HLB peel ethyl acetate extract.

The formation of nanoparticles is indicated by a shift in the wavenumber on the HLB peel nanoparticles. The shift occurred in the peak representing the stretching vibration of the O—H group with a wavenumber of 3 357 cm^{-1} in chitosan, which shifted to 3 198 cm^{-1} in nanoparticles. This is explained by an interaction between the —OH group in chitosan and the —OH group of phenolic compounds in the ethyl acetate extract [37]. Moreover, the N—H bending vibration in chitosan with a wavenumber of 1 591 cm^{-1} shifted to 1 536 cm^{-1} in nanoparticles. This was caused by crosslinking between the NH_2 group of chitosan and NaTPP and the interaction with the phenolic –OH group of phenolic compounds and flavonoids in the ethyl acetate extract [19]. The finding of a peak with a wavenumber of 1 214 cm^{-1} for the nanoparticles indicates the presence of a phosphate group, which is a typical group of NaTPP [38].

Conclusion

This present study revealed that the nanoparticles from the ethyl acetate extract of HLB peels exhibited a stronger antibacterial activity than extracts for which nanotechnology was not applied. The inhibitory effects against *S. aureus* and *E. coli* of ethyl acetate extract of HLB peel were reflected by inhibitory zones of 15.77 and 12.90 mm, respectively, while the corresponding values for the nanoparticles were in the range of 16.28–20.55 mm against *S. aureus* and 14.38–16.58 mm against *E. coli*. Based on the results of characterizing the most active antibacterial nanoparticles, it can be concluded that the secondary metabolites in the HLB ethyl acetate extract were encapsulated by crosslinking between chitosan and NaTPP. Finally, the results strongly suggested that chitosan nanoparticles from the ethyl acetate extract of HLB peels were considered an effective nanomaterial to control bacterial pathogens.

CRediT Author Statement

Wiwik Susanah Rita: Conceptualization, data curation, investigation, writing, editing, and funding acquisition. **Ni Kadek Linda Erika Yanti**: Investigation, methodology, project administration, visualization, and writing-original draft. **I. Made Dira Swantara**: Data curation, supervision, formal analysis, writing, and editing.

Acknowledgment

This research was supported by DIPA PNBP Udayana University FY-2021 in accordance with Research Implementation Assignment Agreement Number B/96-225/UN14.4.A/PT.01.05/2021 (May 3, 2021).

Conflict of Interest

The authors declare that they have no competing interests.

References

[1] S.W. Maya, G. Citraningtyas, W.A. Lolo. Phytochemical screening and antipyretic effect of stem juice from kepok banana (*Musa paradisiaca* L) on white male rats stain wistar (*Rattus norvegicus*) induced with DTP-Hb. *Pharmacon*, 2015, 4(1): 21−29.

[2] W.S. Rita, N.K.L.E. Yanti,. W.G. Gunawan. Uji aktivitas antibakteri kulit Pisang Hijau Lumut (*Musa x paradisiaca* L.) terhadap bakteri *Staphylococcus aureus* dan *Escherichia coli* serta identifikasi golongan senyawa metabolit sekunder. *Jurnal Kimia* (*Journal of Chemistry*), 2021, 15(2): 131−139. https://doi.org/10.24843/JCHEM.2021.v15.i02.p02

[3] W.S. Rita, I.M.D. Swantara, I.A.R.A. Asih, et al. Total flavonoid and phenolic contents of n-butanol extract of *Samanea saman* leaf and the antibacterial activity towards *Escherichia coli* and *Staphylococcus aureus*. *AIP Conference Proceedings*, 2016, 1718(1): 060005. https://doi.org/10.1063/1.4943327

[4] R.L Vifta, F.P. Luhurningtyas. Nanoparticle from *Medinilla speciosa* with Various of encapsulating agent and their antioxidant activities using ferric reducing assay. *Indonesian Journal of Cancer Chemoprevention*, 2020, 11(1): 22−29. https://doi.org/10.14499/indonesianjcanchemoprev11iss1pp22-29

[5] A.P. Bhosale, A. Patil, M. Swami. Herbosomes as a novel drug delivery system for absorption enhancement. *World Journal of Pharmacy and Pharmaceutical Sciences*, 2016, 5: 345−355.

[6] R. Sharma, J. Hazra, P.K. Prajapati. Nanophytomedicines: A novel approach to improve drug delivery and pharmacokinetics of herbal medicine. *Bio Bulletin*, 2017, 3: 132−135.

[7] N. Nurmalia, Y. Sedarnawati, Y. Sri. Sintesis nanopartikel ekstrak kulit manggis merah Dan kajian sifat fungsional produk enkapsulasinya. *Jurnal Teknologi Dan Industri Pangan*, 2017, 28(1): 27−35. https://doi.org/10.6066/jtip.2017.28.1.27

[8] A. Verma, S.P. Gautam, K.K. Bansal, et al. Review green nanotechnology: Advancement in phytoformulation research. *Medicines*, 2019, 6(1): E39. https://doi.org/10.3390/medicines6010039

[9] S. Nyoni, E. Muzenda, N. Mukaratirwa-Muchanyereyi. Characterization and evaluation of antibacterial activity of silver nanoparticles prepared from sclerocarya birrea stem bark and leaf extracts. *Nano Biomedicine and Engineering*, 2019, 11(1): 28−34. https://doi.org/10.5101/nbe.v11i1.p28-34

[10] S. Kumar, V. Sharma, J.K. Pradhan, et al. Structural, optical and antibacterial response of CaO nanoparticles synthesized via direct precipitation technique. *Nano Biomedicine and Engineering*, 2021, 13(2): 172−178. https://doi.org/10.5101/nbe.v13i2.p172-178

[11] A. Rampino, M. Borgogna, P. Blasi, et al. Chitosan nanoparticles: Preparation, size evolution and stability. *International Journal of Pharmaceutics*, 2013, 455: 219−228. https://doi.org/10.1016/j.ijpharm.2013.07.034

[12] K. Divya, M.S. Jisha. Chitosan nanoparticles preparation and applications. *Environmental Chemistry Letters*, 2018, 16: 101−112. https://doi.org/10.1007/s10311-017-0670-y

[13] W.S. Rita, I.A.R.A. Asih, I.M.D. Swantara, et al. Antibacterial activity of flavonoids from ethyl acetate extract of milk banana peel (*Musa* x *paradisiaca* L.). *HAYATI Journal of Biosciences*, 2021, 28: 223−231. https://doi.org/10.4308/hjb.28.3.223

[14] D. Fitri, N.Z.W. Kiromah, T.C. Widiastuti. Formulasi dan karakterisasi nanopartikel ektrak etanol daun salam (*Syzygium polyanthum)* pada berbagai variasi komposisi kitosan dengan metode gelasi ionik. *Journal of Pharmaceutical Science and Clinical Research*, 2020, 5(1): 61−69. https://doi.org/10.20961/jpscr.v5i1.39269

[15] J.B. Harborne. Phytochemical Methods: A guide to modern technique of plant analysis. 2nd edition. London: Chapman and Hall, 1996: 37–99. https://doi.org/10.1007/978-94-009-5570-7

[16] A. Saifudin, V. Rahayu, H.Y. Teruna. Standardisasi bahan obat alam. Yogyakarta: Graha Ilmu, 2011: 1–102.

[17] F.U. Sineke, E. Suryanto, S. Sudewi. Penentuan kandungan fenolik dan sun protection factor (SPF) dari ekstrak etanol dari beberapa tongkol jagung (*Zea mays* L.). *PHARMACON Jurnal Ilmiah Farmasi*, 2016, 5: 275−283.

[18] A.D. Susanti, D. Ardiana, G.P. Gumelar, et al. Polaritas pelarut sebagai pertimbangan dalam pemilihan pelarut untuk ekstraksi minyak bekatul dari bekatul varietas ketan (*Oriza Sativa Glatinosa*). In: Proceedings of Simposium Nasional RAPI XI FT UMS, 2012: 8–15.

[19] E. Rismana, S. Kusumaningrum, O. Bunga, et al. Pengujian aktivitas antiacne nanopartikel kitosan-ekstrak kulit buah manggis (Garcinia mangostana). *Media Litbangkes*, 2014, 24(1): 19−27.

[20] M.H. Kafshgar, M. Khorram, M. Khodadoost, et al. Reinforcement of chitosan nanoparticles obtained by an ionic cross-linking process. *Iranian Polymer Journal* (*English Edition*), 2011, 20(5): 445–456. https://doi.org/10.1016/j.carbpol.2020.116878

[21] T.D. Lam, V.D. Hoang, L.N. Lien. Synthesis and characterization of chitosan nanoparticles used as drug carrier. *Journal of Chemistry*, 2006, 4: 104−109.

[22] M.T. Qurashi, H.S. Blair, S.J. Allen. Studies on modified chitosan membranes. I. Preparation and characterization. *Journal of Applied Polymer Science*, 1992, 46(2): 255−261. https://doi.org/10.1002/app.1992.070460206

[23] R.S. Greco, F.B. Prinz, R.L. Smith. Nanoscale technology in biological system. Boca Raton: CRC Press, 2002: 42–58. https://doi.org/10.1201/9780203500224

[24] Y.Q. Zhang, M.L. Tao, W.D. Shen, et al. Immobilization of L-asparaginase on the microparticles of the natural silk sericin protein and its characters. *Biomaterials*, 2004, 25(17): 3751−3759. https://doi.org/10.1016/j.biomaterials.2003.10.019

[25] Y. Liu, L. Zou, L. Ma, et al. Synthesis and pharmacological activities of xanthone derivatives as α-glucosidase inhibitors. *Bioorganic & Medicinal Chemistry*, 2006, 14(16): 5683−5690. https://doi.org/10.1016/j.bmc.2006.04.014

[26] K.T. Dewandri, S. Yuliani, S. Yasni. Ekstraksi dan karakterisasi nanopartikel ekstrak sirih merah (*Piper crocatum*). *Jurnal Penelitian Pascapanen Pertanian*, 2017, 10(2): 58−65. https://doi.org/10.21082/jpasca.v10n2.2013.58-65

[27] P. Singh, Y.-J. Kim, D.B. Zhang, et al. Review biological synthesis of nanoparticles from plants and microorganisms. *Trends in Biotechnology*, 2016, 34: 588−599. https://doi.org/10.1016/j.tibtech.2016.02.006

[28] D.S.M. Ayumi. Pembuatan dan Karakterisasi nanopartikel ekstrak etanol daun ekor naga (*Rhaphidophora pinnata* (L.f.) Schott) menggunakan

metode gelasi ionik. *Journal of Pharmaceutical Science and Clinical Research*, 2020, 1: 61−69.
[29] A.F. Tomaz, S.M.S. de Carvallo, R.C. Barbosa, et al. Ionically crosslinked chitosan membranes used as a drug carriers for cancer therapy application. *Materials*, 2018, 11: 1−18. https://doi.org/10.3390/ma11102051
[30] A.H. Saberi, Y. Fang, D. McClements. Fabrication of vitamin e-enriched nanoemulsions: Factors affecting particle size using spontaneous emulsification. *Journal of Colloid Interface Science*, 2013, 391: 95−102. https://doi.org/10.1016/j.jcis.2012.08.069
[31] A.Y. Mardani, H. Supriyono. Kajian Produksi Nanopartikel dari Arang Akasia dengan Tumbukan Bola Baja Diameter 5/16, 1/4., 3/16, 5/32 Inchi. UNSPECIFIED Thesis. Publikasi Ilmiah Universitas Muhammadiyah Surakarta, 2018.
[32] Q.G. Liu, Y.Q. Jing, C.P. Han, et al. Encapsulation of curcumin in zein/caseinate/sodium alginate nanoparticles with improved physicochemical and controlled release properties. *Food Hydrocolloids*, 2019, 93: 432−442. https://doi.org/10.1016/j.foodhyd.2019.02.003
[33] V. Nurviana. The potential antioxidant of nanoparticle of limus (Mangifera foetida Lour) seed kernel extract. *Jurnal Farmasi Udayana*, 2020, 9(3): 144–151. https://doi.org/10.24843/JFU.2020.v09.i03.p02
[34] M. Srivastava. High-performance thin-layer chromatography (HPTLC). Berlin, Heidelberg: Springer, 2011. https://doi.org/10.1007/978-3-642-14025-9
[35] N. Duraisamy, S. Dhayalan, M.R. Shaik, et al. Green synthesis of chitosan nanoparticles using of *Martynia annua* L. ethanol leaf extract and their antibacterial activity. *Crystals*, 2022, 12(11): 1550. https://doi.org/10.3390/cryst12111550
[36] I. Antasionasti, I. Jayanto, S.S. Abdullah, et al. Karakterisasi nanopartikel ekstrak etanol kayu manis (*Cinnamomum burmanii*) dengan kitosan sodium tripolifosfat sebagai kandidat antioksidan. *Chemistry Progress*, 2020, 13(2): 77–85. https://doi.org/10.35799/cp.13.2.2020.31392
[37] A.I. Putri, A. Sundaryono, I.N. Chandra. Karakterisasi nanopartikel kitosan ekstrak daun ubijalar (*Ipomoea batatas* L.) menggunakan metode gelasi ionik. *Alotrop*, 2019, 2(2): 203−207. https://doi.org/10.33369/atp.v2i2.7561(sameasRef.[19]
[38] D.L. Pavia, G.M. Lampman, G.S. Kriz, et al. Introduction to spectroscopy. 5th edition. Cengage Learning, 2014: 45–47.

© The author(s) 2023. This is an open-access article distributed under the terms of the Creative Commons Attribution 4.0 International License (CC BY) (http://creativecommons.org/licenses/by/4.0/), which permits unrestricted use, distribution, and reproduction in any medium, provided the original author and source are credited.